

## **Detection of energetic equivalence depends on food web architecture and estimators of energy use**

Poppy Joaquina Romera<sup>1,2\*</sup>, Benoit Gauzens<sup>3,7</sup>, Ana Carolina Antunes<sup>3</sup>, Ulrich Brose<sup>3,7</sup>, Nico Eisenhauer<sup>3,4</sup>, Olga Ferlian<sup>3,4</sup>, Myriam R. Hirt<sup>3,7</sup>, Malte Jochum<sup>3,4,6</sup>, Grace Mitchell<sup>5</sup>, David Ott<sup>12</sup>, Anton Potapov<sup>3,10,11</sup>, Bibishan Rai<sup>1</sup>, Stefan Scheu<sup>8,9</sup>, Kiri Joy Wallace<sup>1,2</sup>, Andrew D. Barnes<sup>1,2</sup>

<sup>1</sup> Te Tumu Whakaora Taiao – Environmental Research Institute, Te Whare Wānanga o Waikato – University of Waikato, Hamilton 3240, New Zealand

<sup>2</sup> Te Aka Mātuatua – School of Science, Te Whare Wānanga o Waikato – University of Waikato, Private Bag 3105, Hamilton, New Zealand

<sup>3</sup> German Centre of Integrative Biodiversity Research (iDiv), Halle–Jena–Leipzig, Puschstraße 4, 04103 Leipzig, Germany

<sup>4</sup> Institute of Biology, Leipzig University, Puschstraße 4, 04103 Leipzig, Germany

<sup>5</sup> Manaaki Whenua – Landcare Research, Private Bag 3127, Waikato Mail Centre, Hamilton 3240, New Zealand

<sup>6</sup> Department of Global Change Ecology, Biocentre, University of Würzburg, Emil–Hilb–Weg 22, 97074 Würzburg, Germany.

<sup>7</sup> Institute of Biodiversity, Friedrich Schiller University Jena, Jena, Germany

<sup>8</sup> JFB Institute of Zoology and Anthropology, University of Göttingen, Untere Karspüle 2, 37073 Göttingen, Germany

<sup>9</sup> Centre of Biodiversity and Sustainable Land Use, University of Göttingen, Büsgenweg 1, 37077 Göttingen, Germany

<sup>10</sup> Senckenberg Museum for Natural History Görlitz, D–02826, Görlitz, Germany

<sup>11</sup> International Institute Zittau, TUD Dresden University of Technology, 02763 Zittau, Germany

<sup>12</sup> Centre for Biodiversity Monitoring and Conservation Science, Leibniz–Institute for the Analysis of Biodiversity Change (LIB), Adenauerallee 127, 53113 Bonn, Germany

**Emails:**

Poppy Joaquina Romera: [poppyromera@gmail.com](mailto:poppyromera@gmail.com) (0009-0001-8110-4623)

Benoit Gauzens: [benoit.gauzens@idiv.de](mailto:benoit.gauzens@idiv.de) (0000-0001-7748-0362)

Ana Carolina Antunes: [ana\\_carolina.antunes@idiv.de](mailto:ana_carolina.antunes@idiv.de) (0009-0003-2909-6106)

Ulrich Brose: [ulrich.brose@idiv.de](mailto:ulrich.brose@idiv.de) (0000-0001-9156-583X)

Nico Eisenhauer: [nico.eisenhauer@idiv.de](mailto:nico.eisenhauer@idiv.de) (0000-0002-0371-6720)

Olga Ferlian: [olga.ferlian@idiv.de](mailto:olga.ferlian@idiv.de) (0000-0002-2536-7592)

Myriam R. Hirt: [myriam.hirt@idiv.de](mailto:myriam.hirt@idiv.de) (0000-0002-8112-2020)

Malte Jochum: [malte.jochum@uni-wuerzburg.de](mailto:malte.jochum@uni-wuerzburg.de) (0000-0002-8728-1145)

Grace Mitchell: [graceimitchell@hotmail.com](mailto:graceimitchell@hotmail.com) (0000-0002-2839-7981)

David Ott: [d.ott@leibniz-lib.de](mailto:d.ott@leibniz-lib.de) (0000-0001-7079-3411)

Anton Potapov: [anton.potapov@idiv.de](mailto:anton.potapov@idiv.de) (0000-0002-4456-1710)

Bibishan Rai: [br62@students.waikato.ac.nz](mailto:br62@students.waikato.ac.nz)

Stefan Scheu: [sscheu@gwdg.de](mailto:sscheu@gwdg.de) (0000-0003-4350-9520)

Kiri Joy Wallace: [kiri.wallace@waikato.ac.nz](mailto:kiri.wallace@waikato.ac.nz) (0000-0003-1236-6846)

Andrew D. Barnes: [andrew.barnes@waikato.ac.nz](mailto:andrew.barnes@waikato.ac.nz) (0000-0002-6499-381X)

**\*Corresponding Author:** Poppy Joaquina Romera

**Short running title:** Energetic equivalence in soil food webs

**Key words:** Metabolic Theory of Ecology, community assembly, body size, abundance, scaling, soil invertebrates, metabolism, energy flux.

**Type of Article:** Letter

**Statement of authorship:** PJR and ADB conceived the study. PJR, ADB, AP, BR, GM, KJW, MJ, and OF collected and processed the soil data. ACA curated and processed the EFForTS and ECOWORM soil data. PJR and BG analysed the data. PJR and ADB wrote the first draft of the manuscript, and all authors contributed substantially to revisions.

**Data accessibility statement:** Data and code supporting the results have been archived in appropriate public repositories. Code DOI: [10.6084/m9.figshare.25591227](https://doi.org/10.6084/m9.figshare.25591227) and data DOI: [10.6084/m9.figshare.25591254](https://doi.org/10.6084/m9.figshare.25591254). All data from the EFForTS and ECOWORM project can be requested by contacting the corresponding author of Antunes et al. (2023).

**Number of words in Abstract:** 145

**Number of words in main text:** 4980

**Number of references:** 38

**Number of tables:** 0

**Number of figures:** 6

## Abstract

Ecologists have long debated the universality of the energetic equivalence rule (EER), which posits that population energy use should be invariant with average body size due to negative size–density scaling. We explored size–density and size–energy use scaling across 183 geographically–distributed soil invertebrate food webs to investigate the universality of these fundamental EER assumptions. Additionally, we compared two measures of energy use to investigate size–energy use relationships: population metabolism and energy fluxes. We found that size–density scaling did not support energetic equivalence in soil communities. Furthermore, evidence of energetic equivalence was dependent on the estimate of energy use applied (population metabolism or energy flux), the trophic level of consumers, and food web properties. Our study demonstrates a need to integrate food web energetics and trophic structure to better understand how energetic constraints shape the body size structure of terrestrial ecosystems.

## Introduction

The power–law scaling of body size with organism metabolism and abundance are some of the most widely observed, studied, and debated biological relationships (Hatton et al. 2019). Scaling relationships can describe and explain fundamental energetic constraints that determine the structure and functioning of ecological communities, but this is heavily contingent on the underlying expectations of these scaling relationships, as well as the variables used to describe them. Specifically, the Metabolic Theory of Ecology (MTE) predicts that 1) the energy use of an individual organism  $i$  ( $E_i$ ) scales with whole–organism body size  $M_i$  with a positive  $\frac{3}{4}$  (0.75) exponent ( $E_i \propto M_i^{0.75}$ ), and 2) the abundance (i.e., density)  $N$  of individuals scales with population body size  $M$  with a negative  $\frac{3}{4}$  (–0.75) exponent ( $N \propto M^{-0.75}$ ). Therefore, population  $n$  energy use (hereafter,  $E_n$ , the total energy

consumption required to support population  $n$  biomass) should be invariant with respect to population–average body size (that is,  $E_n \propto M_n^0$ ; Brown et al. 2004; Damuth, 1987; White et al. 2007). This is known as the energetic equivalence rule (EER) and is one of the central expectations of the MTE (Brown et al. 2004; White et al. 2007). Yet, there is still considerable discord around the generality of the EER applying across natural ecosystems, which partly stems from observed variation in the underlying biological assumptions of the EER, as well as variation in approaches used to estimate body size and energy use relationships of communities.

A zero exponent of the scaling relationship between the body size and energy use of all populations in a given community (i.e.,  $E_n \propto M_n^0$ ) is only met if whole organism body size–energy use (i.e.,  $E_i \propto M_i$ ) and size–density ( $N \propto M$ ) inverse relationships have opposite exponent values (e.g.,  $E_i \propto M_i^{0.75}$  and  $N \propto M^{-0.75}$ ; Brown et al. 2004). While numerous studies have found a  $-0.75$  size–density scaling exponent ( $N \propto M^{-0.75}$ ) among populations within communities (e.g., Damuth, 1987; Hatton et al. 2019; Meehan, 2006b; Meehan et al. 2006), many others have found considerable variation around this expected scaling across major taxonomic groups (Ehnes et al. 2011; Glazier, 2022; Hatton et al. 2019; Ott et al. 2014a; Ott et al. 2014b; Savage et al. 2004). Nevertheless, an expectation of a  $-0.75$  exponent is still widely employed (Hatton et al. 2019). Observed deviations from a  $-0.75$  size–density exponent within communities can arise from variation in the allometric exponent of basal metabolic rates across taxa, but also from varying energetic constraints across trophic levels, life history traits, and environmental conditions (Antunes et al. 2023; Hatton et al. 2019). Despite the fundamental assumptions of the EER, few studies have tested for both size–density and size–energy use relationships to detect energetic equivalence (Damuth, 1987; Ehnes et al. 2014; Meehan, 2006a), and most assume energetic equivalence based only on

size–density ( $N \propto M^{-0.75}$ ) and/or whole-organism body size–energy use ( $E_i \propto M_i^{0.75}$ ) scaling (Damuth, 1981; Meehan, 2006b; Meehan et al. 2006).

In addition to variation across taxa, size–density and size–energy use scaling relationships should vary systematically across trophic levels (Fig. 1; Brown et al. 2004; Trebilco et al. 2013). Food webs comprise populations receiving energy from a common energy or basal resource pool (Trebilco et al. 2013). Energy captured from primary consumers at the lowest trophic level is transferred inefficiently to secondary consumers at higher trophic levels, ultimately leading to the bottom–heavy food web structures predicted by the MTE (i.e., highly abundant, small–bodied versus less abundant, larger–bodied organisms; Potapov et al. 2019a; Trebilco et al. 2013). This means that predator–prey relationships and the efficiency of trophic energy transfer are key factors that determine the form of size–density and, consequently, size–energy use power law relationships across and within trophic levels of food webs. Due to the inefficient transfer of energy from a resource to its consumer, food webs exhibit a decrease in energy availability with increasing trophic level and body size (Trebilco et al. 2013). Therefore, the scaling of size–density and size–energy use should be  $N \propto M^{<-0.75}$  (i.e., more negative than  $-0.75$ , Fig. 1a) and  $E_n \propto M_n^{<0}$  (i.e., more negative than zero, Fig. 1b), respectively, across all trophic levels, compared with  $N \propto M^{-0.75}$  and  $E_n \propto M_n^0$  within single trophic levels (Trebilco et al. 2013) because they share the same energy pool (White et al. 2007). However, since secondary consumers are made up of multiple trophic levels that do not access the basal resource pool directly, they should have the steepest size–density and size–energy use scaling exponents as they have greater energetic constraints (Fig. 1a, b; Trebilco et al. 2013). These systematic deviations from expected scaling exponents that relate to trophic positioning of species question the theoretical foundation of the EER and call for a food web perspective.

A paramount challenge in describing size–energy use scaling relationships is the ability to accurately assess energy use of populations in food webs. While this has typically been achieved by quantifying population metabolism (the summed metabolic rates of organisms within a population), this approach does not consider additional energetic expenditure due to the inefficiency of trophic energy transfer, losses to predation from higher trophic levels, and other trophic–level–dependent variation in energy loss (Brown et al. 2004). Alternative measures such as trophic energy flux account for total transfer of energy in and out of a population and can, therefore, describe the total energetic losses (and thus expenditure) due to metabolism, assimilation efficiency, and consumption by higher trophic levels (i.e., predation; Barnes et al. 2018; Gauzens et al. 2019). These losses must be balanced by the energetic gains of an organism (i.e., maintenance of energy balance), and are, therefore, directly related to energy use of a population (Barnes et al. 2018). Thus, measures of total energy consumption (i.e., influx of energy into a given food web node before assimilation) should provide a more precise estimate of population energy use compared to population metabolism, which can be integrated into analyses of size–energy use scaling relationships (Fig.1; Gauzens et al. 2019). An energy flux approach will allow to better address the paradox of the EER that expectations should mostly hold within trophic levels, but with systematic deviations across trophic levels.

Here we analysed size–density ( $N \propto M$ ) and size–energy use ( $E_n \propto M_n$ ) scaling in soil invertebrate food webs across four geographical locations to investigate the universality of size–density scaling relationships and their likelihood of accurately indicating energetic equivalence in soil communities of primary and secondary consumers. Additionally, we compared two measures of energy use to investigate size–energy use relationships: population metabolism ( $I_n \propto M_n$ ) and energy fluxes ( $F_n \propto M_n$ ). We hypothesised that (1)  $N \propto M$  and  $E_n \propto M_n$  scaling across all trophic levels (i.e., entire food webs) would be more negative

than the MTE expectations of scaling exponents (i.e.,  $N \propto M^{<-0.75}$  and  $E_n \propto M_n^{<0}$ ) due to inefficiencies in energy transfer from consumption. We also expected that (2)  $N \propto M^{-0.75}$  and  $E_n \propto M_n^0$  scaling would be seen within trophic levels because individuals within these guilds feed from the same resource base, whereas secondary consumers will be less likely to meet  $N \propto M^{-0.75}$  and  $E_n \propto M_n^0$  expectations as they are more constrained by competition within food webs compared to primary consumers that only consume basal resources (Trebilco et al. 2013). However, we also hypothesised that (3)  $E_n \propto M_n$  scaling using metabolism  $I$  as an estimate of energy use will be less likely to produce scaling exponents that meet expectations compared to energy flux  $F$ , as metabolism does not account for additional energetic expenditure due to assimilation (in)efficiency and losses to predation by higher trophic level consumers.

## **Material and methods**

### **Soil invertebrate community sampling**

Soil invertebrate community data was collected from four locations (Aotearoa New Zealand, Indonesia, Canada, and U.S.A) through sampling efforts of three large-scale projects (Fig. 2). (1) The Aotearoa New Zealand plots (People Cities & Nature programme) were established in forest patches within nine cities spanning  $\sim 9^\circ$  of latitude (Fig. 2, Table S1). These were part of a 60-year-old planted and primary old-growth urban forest chronosequence (n=73). (2) The Indonesian (EFForTS project) study plots (n=30, Fig. 2) were established in remnant tropical rainforest, jungle rubber agroforest systems, rubber monocultures, and oil palm monocultures across two landscapes surrounding Bukit Duabelas and Harapan rainforest reserves in the Jambi Province, Sumatra, Indonesia (Antunes et al. 2023; Drescher et al. 2016). The ECOWORM project study plots (n=80, Fig. 2) in (3) the United States (St John's forest, Minnesota) and (4) Canada (Barrier Lake North, Barrier Lake South, and Bull Creek

Hills in the Canadian Rocky Mountains, Kananaskis Valley, Alberta) were established in maple and aspen forest sites, respectively, whereby each of these forests contained a low–invasion and a high–invasion exotic earthworm area–per forest (10 plots in low– and 10 plots in high–invasion areas; Antunes et al. 2023; Jochum et al. 2021).

### **Soil invertebrate community data collection and preparation**

Aotearoa New Zealand soil invertebrates were sampled between November 2019–February 2020 (austral summer) from three 50 × 50 cm subplots by taking one macrofauna soil core (22 cm diameter, 10 cm deep from the mineral soil layers) and one mesofauna soil core (5 cm diameter, 10 cm deep mineral soil layers) per subplot. Macro– and mesofauna were extracted from the soil cores using heat extraction and identified in the laboratory to family or order level (Naumann, 1991). Individual body length (mm) was converted to fresh body size (mg) using length–size scaling relationships according to different invertebrate phylogenetic groups from published literature (Table S2; Barnes et al. 2014; Mercer et al. 2001; Sohlström et al. 2018). Soil invertebrate collection from all other geographic regions followed similar procedures, whereby mesofauna were collected either from small cores (5 cm diameter, 10 cm deep) or 16 cm x 16 cm quadrats (5 cm deep), and macrofauna were collected from large soil cores (20 cm diameter, 10 cm deep), leaf litter sieving (0.5 m<sup>2</sup> ECOWORM and 1m<sup>2</sup> EFForTS), and mustard extraction for earthworms (0.25 m<sup>2</sup>). For more detailed methods see Antunes et al. (2023).

To analyse size–energy use relationships, we took the natural logarithm of all body sizes and grouped them into 0.25 log(mg) size class bins. We took the median of natural logarithm body size of each size class bin per plot. Abundance was then calculated as the number of individuals in each size class bin per plot and scaled to 1 m<sup>2</sup>. For analysing size–density relationships, the counts of soil invertebrate fresh body sizes (mg) were scaled up to 1

m<sup>2</sup>. We calculated individual metabolic rates  $I$  (J hr<sup>-1</sup>) for invertebrates within each taxonomic group (see Table S3 for regressions applied to each taxon) using the following equation from (Ehnes et al. 2011).

$$1) I = \exp(\ln(i_0) + \alpha \times \ln(M) - E / (k \times T)).$$

Where  $k$  is Boltzmann's constant ( $8.62 \times 10^{-5}$ ),  $T$  is environmental temperature in Kelvin,  $E$  the activation energy,  $i_0$  the taxa specific normalisation constant and,  $\alpha$  is the allometric exponent. Plot-level mean annual soil temperature was collected using data loggers and local area-level annual soil temperature from online weather databases (National Oceanic and Atmospheric Administration n.d.). We took the natural logarithm of individual invertebrate metabolic rates, summed per size class bin per plot, and scaled to 1 m<sup>2</sup>.

### **Food web reconstruction and consumer energy intake calculation**

To reconstruct soil food webs, food web nodes were defined according to organism taxonomic order (or family level for Hymenoptera and Coleoptera) for which information on their general feeding preferences was obtained. We constructed a meta-matrix of binary consumer-resource interactions, whereby feeding links were assigned based on feeding preferences obtained from literature (Naumann, 1991; Potapov et al. 2022). Energy influx in J day<sup>-1</sup> into each consumer node within a local food web (i.e., plot) was calculated using the food-web energetics approach as described by Barnes et al. (2018) and Gauzens et al. (2019) to quantify the energy intake of organisms across the 183 local food webs. To calculate energy fluxes, we assumed that losses in energy from consumer nodes (via metabolism and predation) were balanced by intake of energy through resource consumption (taking assimilation efficiency into account; Barnes et al. 2020; Gauzens et al. 2019). For full methods for the calculation of energy flux (i.e., consumer energy intake) and metabolism, see supplementary information.

Because body size was grouped into size class bins (irrespective of food web node) per plot to analyse size–energy relationships and energy flux was calculated per food web node per plot ( $F_{node}$ ), to attribute the proportion of ingoing energy flux from each food web node to each size class bin per plot ( $F_{size\ class}$ ), we calculated proportional energy flux according to the summed metabolism of each size class ( $I_{size\ class}$ ) and energy intake of that node as:

$$2) F_{size\ class} = I_{size\ class} \times F_{node} / I_{fw}$$

Where  $I_{fw}$  is the summed metabolism of all size classes in a food web. Energy fluxes were then natural logarithm–transformed and scaled to  $1\text{m}^2$ .

For each local food web, we further determined mean trophic similarity among node, prey–averaged trophic level, observed node richness, and trophic level omnivory (see supplementary for full methods).

### **Statistical analysis**

To analyse size–density relationships ( $N \propto M$ ) across whole soil invertebrate food webs and within primary and secondary consumers, we used maximum likelihood estimation (MLE) to estimate the exponent  $b$  derived from individual size distributions (ISD) of all individual body sizes (scaled to  $1\text{m}^2$ ) within soil invertebrate communities using the sizeSpectra package in R (see Edwards et al. 2017). To check the fit of models against observed body size data ( $x$ ), rank–frequency plots were produced giving the natural logarithm–rank of the number of observations  $\geq x$  against the value of  $x$  (Edwards et al. 2017; See supplementary code to perform MLE model checks).

To analyse size–metabolism ( $I_n \propto M_n$ ), and size–energy flux ( $F_n \propto M_n$ ) scaling relationships across whole soil invertebrate food webs and within primary and secondary consumers, we used ordinary least squared (OLS) regression using log median body mass data (scaled to  $1\text{m}^2$ ). Ranged major axis regression was also used to model size–energy use

relationships to check against OLS methods for sensitivity of results to model fitting approach (see supplementary information for full methods). MLE and OLS regression models were run across all communities (i.e., plots) within the four geographic regions. We excluded all resulting models with less than 10 body size class bins or individuals per food web from our analysis due to insufficient data for estimating reliable model fits. As a result, our analyses yielded a total of 183 food webs (i.e., comprising both primary and secondary consumers) and 355 trophic level models (173 models for primary consumers and 179 for secondary consumer food webs).

Additionally, we investigated whether the likelihood of size–density and size–energy use relationships to meet EER expectations could be explained by variation in food web structure. To do so, for all food webs, we constructed a normal linear model testing for the response of the absolute log–deviation of observed exponents from expected size–energy use exponents ( $I_n \propto M_n^0$  and  $F_n \propto M_n^0$ ) to omnivory, node richness, and trophic similarity per food web and per trophic level (i.e., primary and secondary consumers). This produced six linear models in total. All statistical analyses were performed in R version R 4.4.0 (R Core Team, 2023).

## Results

Scaling exponents of soil invertebrate consumers across all trophic levels in soil food webs were, on average, more negative than expected for size–density relationships (i.e.,  $N \propto M^{<-0.75}$ , mean =  $-1.174$ , median =  $-1.152$ ) and less negative than expected for size–metabolism (i.e.,  $I_n \propto M_n^{>0}$ , mean =  $0.134$ , median =  $0.164$ ) and size–energy flux (i.e.,  $F_n \propto M_n^{>0}$ , mean =  $0.204$ , median =  $0.195$ ) relationships (Fig. 3). Nevertheless, exponents for both measures of energy use ( $I_n \propto M_n$  and  $F_n \propto M_n$ ) appeared to have a similar central tendency around exponents expected by the MTE, as indicated by kurtosis values of four. Overall, we found that 1.1% of

all soil food webs contained  $-0.75$  within the confidence interval of exponent estimates, therefore, meeting size–density expectations (Fig. 3a). Metabolism as an estimate of energy use appeared to better fit EER expectations compared to energy flux, as 50.3% of all soil food webs met scaling expectations for size–metabolism relationships (Fig. 3b) compared to 41.5% for size–energy flux relationships (Fig. 3c).

There was a significant positive effect of node richness on the deviation of food webs from the hypothesised size–metabolism exponent ( $p < 0.01$ , Fig. 4a, Table S4), whilst it had a significant negative effect on the deviation of food webs from the hypothesised size–energy flux exponent ( $p < 0.01$ , Fig. 4d, Table S4). In contrast, we found a significant negative effect of trophic similarity on the deviation of food webs from both the hypothesised size–metabolism ( $I_n \propto M_n^0$ ) and size–energy flux ( $F_n \propto M_n^0$ ) exponents ( $p < 0.01$ , Fig. 4b,e, Table S4). Overall, there appeared to be no significant effect of food web omnivory on the deviation of soil food webs from predicted  $I_n \propto M_n^0$  or  $F_n \propto M_n^0$  exponent values (Fig. 4c, f).

Similar to the trends observed in EER scaling relationships observed for whole food webs, scaling relationships for primary consumers produced exponents that were, on average, more negative than expected for size–density relationships ( $N \propto M^{<-0.75}$ , mean =  $-1.191$ , median =  $-1.109$ ) and more positive than expected for size–metabolism ( $I_n \propto M_n^{>0}$ , mean =  $0.261$ , median =  $0.268$ ) and size–energy flux ( $F_n \propto M_n^{>0}$  mean =  $0.761$ , median =  $0.646$ ) relationships (Fig. 5a,b,c). As predicted, secondary consumer scaling exponents were, on average, more negative than expected for size–density ( $N \propto M^{<-0.75}$ , mean =  $-1.218$ , median =  $-1.201$ ), size–metabolism ( $I_n \propto M_n^{<0}$ , mean =  $-0.039$ , median =  $-0.003$ ) and size–energy flux ( $F_n \propto M_n^{<0}$ , mean =  $-0.394$ , median =  $-0.524$ ) relationships (Fig. 5d,e,f). Out of 173 primary consumer communities, 15% met expectations for size–density ( $N \propto M^{<-0.75}$ ), 42.9% met size–metabolism ( $I_n \propto M_n^0$ ), and 46.3% met size–energy flux ( $F_n \propto M_n^0$ ) scaling expectations. Comparatively, out of 180 secondary consumer communities, 1.7% met size–density ( $N \propto M^{<-0.75}$ ), 42.9% met size–metabolism ( $I_n \propto M_n^0$ ), and 46.3% met size–energy flux ( $F_n \propto M_n^0$ ) scaling expectations.

<sup>0.75</sup>), 41.4% met size–metabolism ( $I_n \propto M_n^0$ ), and 54.1% met size–energy flux ( $F_n \propto M_n^0$ ) scaling expectations. We also found less variation (i.e., higher kurtosis of the respective density functions for scaling exponent estimates) around the mean and median exponents for the scaling of body size with energy fluxes ( $F_n \propto M_n$ ) compared to metabolism ( $I_n \propto M_n$ ) for secondary consumers, and vice versa for primary consumers. In line with our expectations, we found that mean and median exponent values for  $I_n \propto M_n$  and  $F_n \propto M_n$  relationships were closer to zero for secondary consumers than for primary consumers.

We only found a significant positive effect of trophic similarity within secondary consumer food webs on the deviation from size–metabolism scaling expectations ( $I_n \propto M_n^0$ , Fig. 6b). In contrast, for size–energy use scaling based on energy fluxes, we found a significant positive effect of node richness and a significant negative effect of trophic similarity and omnivory on the deviation from size–energy flux scaling expectations for secondary consumers ( $F_n \propto M_n^0$ ,  $p < 0.01$ , Fig. 6d,e,f, Table S4). However, we found no significant effects of node richness or trophic similarity on deviations from the size–metabolism or size–energy flux exponents expected by the EER for primary consumers ( $p < 0.05$ , Fig. 6, Table S4).

## Discussion

We found broadly contrasting evidence for energetic equivalence in soil food webs across the 183 sites from four geographic regions. Inference of energetic equivalence was especially variable between scaling exponents from size–density, size–metabolism, and size–energy flux scaling. Very few soil food webs (1.1%) met size–density scaling expectations (i.e., exponent of  $-0.75$ ), whereas 50.3% and 41.5% of food webs also met size–metabolism and size–energy flux expectations (i.e., exponent of zero), respectively (Figs 4, 6; see also Marquet et al. 1995). More than 50% of whole food webs (i.e., across both primary and

secondary consumers, Fig. 3) met EER expectations for size–energy use scaling relationships when using metabolism as an estimate of energy use. This suggests that metabolism better fit EER expectations compared to energy flux at the whole food web level (Fig. 3). Within trophic levels, secondary consumers appeared to be more energetically constrained, likely because they do not directly draw from the basal resource pool. Furthermore, size–energy use scaling relationships using energy flux, on average, resulted in exponents closer to zero expectations for secondary consumer communities (Fig. 5; Trebilco et al. 2013). Our results demonstrate that energy flux produces more precise estimates of energy use for secondary consumer communities, compared with metabolism, and show notable differences in size–density and size–energy use scaling relationships within and across primary and secondary consumer trophic levels. Thus, each scaling relationship presents different crucial pieces of information about the energetic structure of food webs (Trebilco et al. 2013).

We found that 41.5% of whole soil food webs (Fig. 4) met EER expectations (size–energy use exponents of zero) when using energy flux compared to 50.3% for metabolism as an estimate of energy use (which was also supported by RMA model fitting; Fig. S1). In contrast, over 50% of secondary consumer communities (Fig. 6) met EER expectations when using energy flux, compared to 41.4% for metabolism as an estimate of energy use (also qualitatively mirrored by RMA regression results; Fig. S2). However, only 1.1% of whole soil food webs met size–density expectations (Fig. 3), clearly demonstrating that size–density scaling exponents near  $-0.75$  do not necessarily equate to energetic equivalence in ecosystems. Even though size–density scaling is related to energy use within a community, alone, it is unlikely a reliable indicator of energetic equivalence (Ehnes et al. 2014; Potapov et al. 2021). Indeed, our findings suggest that many past studies may have incorrectly assumed a lack of community energetic equivalence based on size–density scaling exponents that do not equal  $-0.75$  (Damuth, 1981; Meehan, 2006b; Meehan et al. 2006). It is important

to note that energetic equivalence and size–density scaling exponents of  $-0.75$  are contingent on a whole organism size–metabolism allometric exponent of  $0.75$ , which is known to be untrue for many taxa (Glazier, 2022; Hatton et al. 2019; Savage et al. 2004) and could be partially responsible for the disparity in findings between size–density and size–energy use exponents. It is likely impossible to understand the energetic structuring, dependent on factors such as metabolic demands, assimilation efficiencies, and losses in energy due to predation (Barnes et al. 2018), by studying the scaling of abundances of organisms with body size alone (Brown et al. 2004). Furthermore, ecosystems at various stages of succession following subsequent natural or human disturbances are unlikely to be at demographic equilibrium as assumed by MTE and, hence, are unlikely to meet EER expectations (Antunes et al. 2023; Brown et al. 2004; Ehnes et al. 2014). Many constraints under natural conditions pose significant challenges to proving energetic equivalence of communities. As such, simplified, controlled experiments are needed where exact energy inputs into the system and individual energy intake within a food web are known.

Our study revealed that energy flux may provide a more precise estimation of the energetic demands within trophic levels, especially for secondary consumers in food webs (Fig. 5). In contrast to metabolism, energy flux captures losses in energy from assimilation and transfer efficiency, in addition to metabolic losses, especially in secondary consumers that experience greater energetic constraints than primary consumers (Polis & Strong, 1996). Primary consumers are also highly dependent on ecosystem-specific primary productivity which varies across ecosystems from sub–arctic, temperate, to tropical regions such as those analysed in our study (Potapov, Klarner, et al. 2019). Compared to metabolism, energy flux may therefore better capture differences in energy use and, ultimately, losses (due to metabolism, assimilation efficiency, and predation) among the geographical locations of our study sites attributable to their varying climate conditions (e.g., temperature). Taken together,

our findings suggest that estimates of energy use other than metabolism are likely required for accurate estimates of trophic level-specific size–energy use scaling relationships and, therefore, the detection of energetic equivalence across ecosystems.

We found that primary consumer food webs had exponents greater than predicted values (i.e.,  $N \propto M^{>-0.75}$ ,  $I_n \propto M_n^{>0}$  or  $F_n \propto M_n^{>0}$ , Fig. 5 & Fig. S2) compared to secondary consumers (conforming with previous findings; e.g., Potapov et al. 2021; Ulrich et al. 2015), which had exponents that were more negative than expected based on EER expectations (i.e.,  $N \propto M^{<-0.75}$ ,  $I_n \propto M_n^{<0}$  or  $F_n \propto M_n^{<0}$ , Fig. 5 & Fig. S2). We argue that this is because primary consumers fall within a single trophic level, directly accessing their energy from a less limiting (i.e., greater biomass) basal resource pool, making them less energetically constrained (see also Trebilco et al. 2013). Additionally, this phenomenon follows the food web subsidy hypothesis where organisms with access to resource subsidies, such as millipedes and earthworms (i.e., primary consumers), will have size–energy use scaling exponents more positive than predicted by the MTE. Primary consumers may also be more size compartmentalised than secondary consumers, allowing for resource subsidisation of large primary consumers and relaxing energetic constraints within food webs (Potapov et al. 2019b). However, the secondary consumers in our study comprised organisms from multiple trophic levels. Because of this trophic structuring of secondary consumers, and indirect access to basal resources, energetic constraints are tightened due to the inefficiency of energy transferred to each higher trophic level (shown by the highly constrained frequency of size–energy flux scaling exponents around mean and median; Fig. 5f). These results support the expectations formulated by Trebilco et al. (2013) that size–energy use scaling across communities made up of multiple trophic levels should be more negative than those within a singular trophic level. The more negative size–density exponents seen in secondary (mean =  $-1.218$ ) versus primary (mean =  $-1.191$ ) consumers are also consistent with the resource–

thinning hypothesis in soil food webs proposed by Ehnes et al. (2014), where the abundance of organisms decreases with body size even more than expected with increasing trophic level because of increasing energetic constraints (Fig 5a, d). Overall, our results suggest that primary consumers (especially larger primary consumers) at the base of food webs are subject to weaker energetic constraints than consumers at higher trophic levels, highlighting the importance of a trophic level-explicit approach to analysing EER scaling relationships (Hechinger et al. 2011; Potapov et al. 2019b).

Past studies have explored sources of variation in EER scaling relationships, but few have investigated the role of food web architecture. We found various food web properties were important predictors of energetic equivalence in soil food webs. Increased node richness of secondary consumers in soil food webs resulted in significantly greater deviations from size–energy flux expectations (Fig. 6), whereas food webs with lower trophic similarity and omnivory of secondary consumers were more likely to meet size–energy flux expectations (Fig. 6). Interestingly, this contrasted with analyses across trophic levels, where deviation from expected size–energy flux exponents decreased with node richness and trophic similarity across trophic levels (Fig. 4). As trophic similarity (and node richness) increases within whole food webs, competition should also increase due to niche overlap (Eisenhauer, 2012; Poisot et al. 2013; Polis & Strong, 1996), which should in turn increase energetic constraints and the likelihood of meeting EER expectations (Trebilco et al. 2013). This is especially true for secondary consumers that are more energetically constrained because they span multiple trophic levels with more variable body sizes, compared to primary consumers (Potapov et al. 2019b). Like our results, Ulrich et al. (2015) found higher trophic levels (predators) were more likely to meet EER expectations compared to decomposers (i.e., primary consumers). In addition, increasing secondary consumer node richness should allow for greater trophic complementarity (Poisot et al. 2013) due to more trophic niches that

support increased niche partitioning (Eisenhauer, 2012; Polis & Strong, 1996). This should relax competition for resources (Eisenhauer, 2012; Polis & Strong, 1996), reducing energetic constraints on secondary consumers and, therefore, observed deviations from size–energy flux expectations. Interestingly, food webs with higher trophic similarity and omnivory of secondary consumers deviated less from size–energy flux expectations. In other words, deviation from EER expectations was greater when node richness was high and trophic similarity and omnivory were low (i.e., high taxonomic and trophic diversity). Deviation from EER expectations in these food webs could be due to especially high niche complementarity and facilitation that could relax energetic constraints, allowing for larger than expected populations for a given body size. Ultimately, our results provide evidence that food webs with more secondary consumer nodes (i.e., greater trophic node diversity) are more diverse in their trophic niches, experience less competition, and may therefore be less likely to meet EER expectations.

Our study raises important questions about our understanding of the transfer of energy within food webs. By employing an energetic food web approach, our study sheds light on systematic variation in energetic constraints across trophic levels. Additionally, our findings raise fundamental questions about the use of size–density scaling to infer energetic equivalence in ecosystems. While metabolism appeared to be a better indicator of energetic equivalence at the whole food web level, energy flux provided a better estimate of energy use for indicating energetic equivalence within trophic levels, especially for secondary consumers. The positive effects of consumer diversity and trophic complementarity on deviation from EER expectations further demonstrated the stronger energetic constraints faced by secondary consumers and the need for a trophic level-explicit approach to testing the EER. Though we found evidence of energetic equivalence across ecosystems, deviations from EER expectations were more frequent, indicating the prevalence of external processes

such as disturbances in non-equilibrium systems that prevent soil food webs from exhibiting properties of energetic equivalence. In this sense, observed deviations from energetic equivalence can facilitate understanding of the underlying mechanisms and energetic constraints driving these deviations. We therefore urge future studies to employ an energetic food web approach that considers trophic structuring and food web energy use to explore energetic equivalence across ecosystems.

### Figures and tables

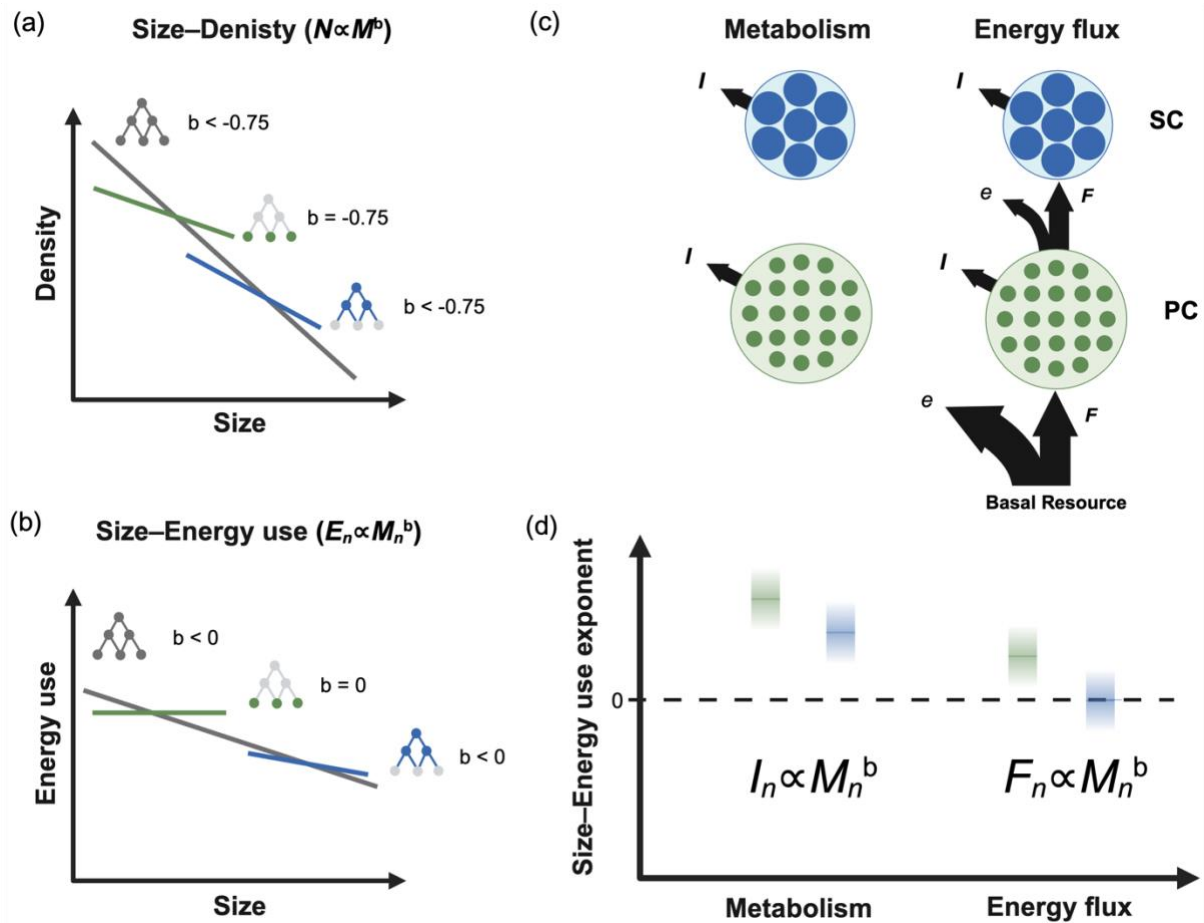


**Figure 1.** Predicted population size–density ( $N \propto M^b$ , (a)) and size–energy use ( $E_n \propto M_n^b$ , (b)) exponents  $b$  across food webs (dark grey line) and within primary consumers (PC, green line) and secondary consumers (SC, blue line). In panel (c) we show population metabolism  $I$  versus population energy flux  $F$  to investigate  $E_n \propto M_n$  scaling for expectations of energetic

equivalence within PC and SC in soil food webs. The size and number of circles within the PC and SC nodes indicate the relative body size and abundances of individuals (i.e., populations of communities). Metabolism only takes into account losses in energy due to metabolism, resulting in an underestimation of size–energy use exponents, whilst energy flux takes into account energetic losses due to metabolism  $I$ , assimilation efficiency  $e$ , and predation on different resources (basal resources or other nodes), causing size–energy use exponents to be more precise (d).

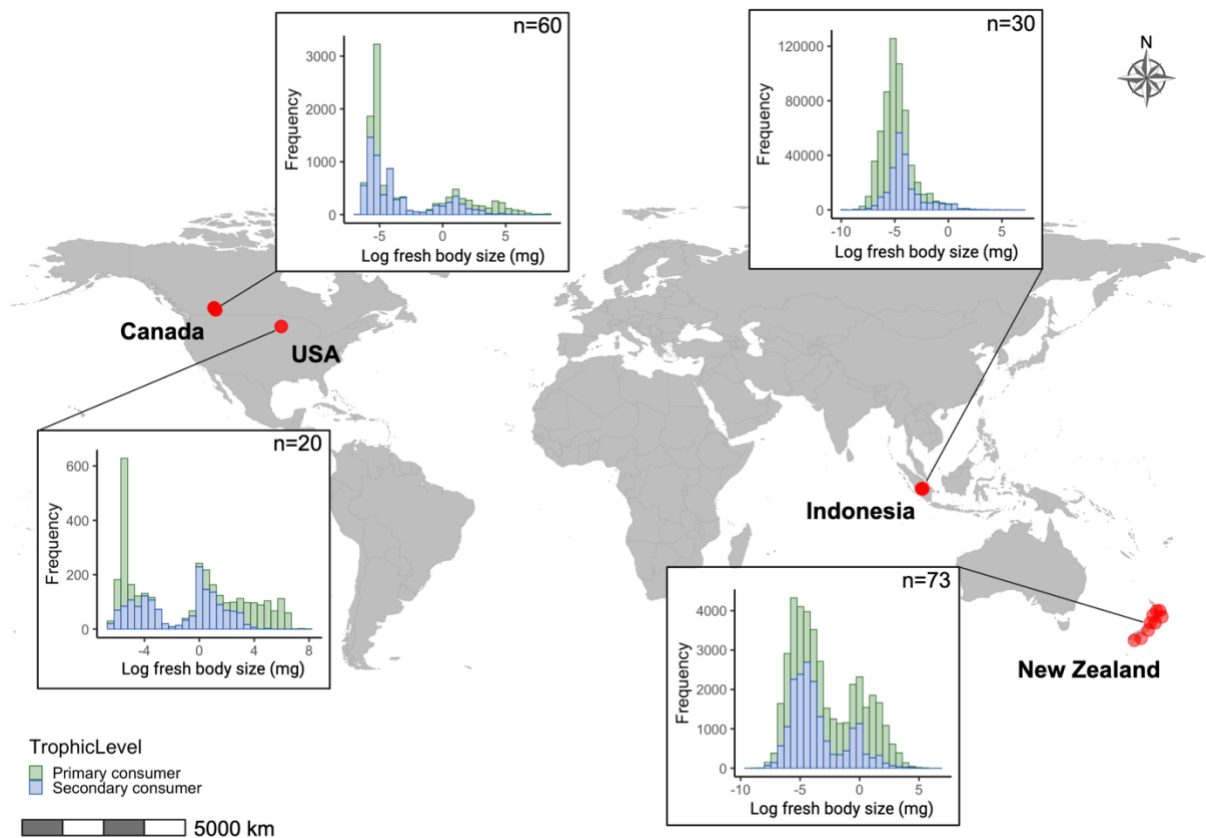


**Figure 2.** Distribution of the 183 plots where soil invertebrate communities were sampled; n is the number of plots (i.e., local communities) within each geographic region. Histograms show the natural logarithm of fresh body size (mg) distributions across primary (green) and secondary (blue) consumers within each geographic region.

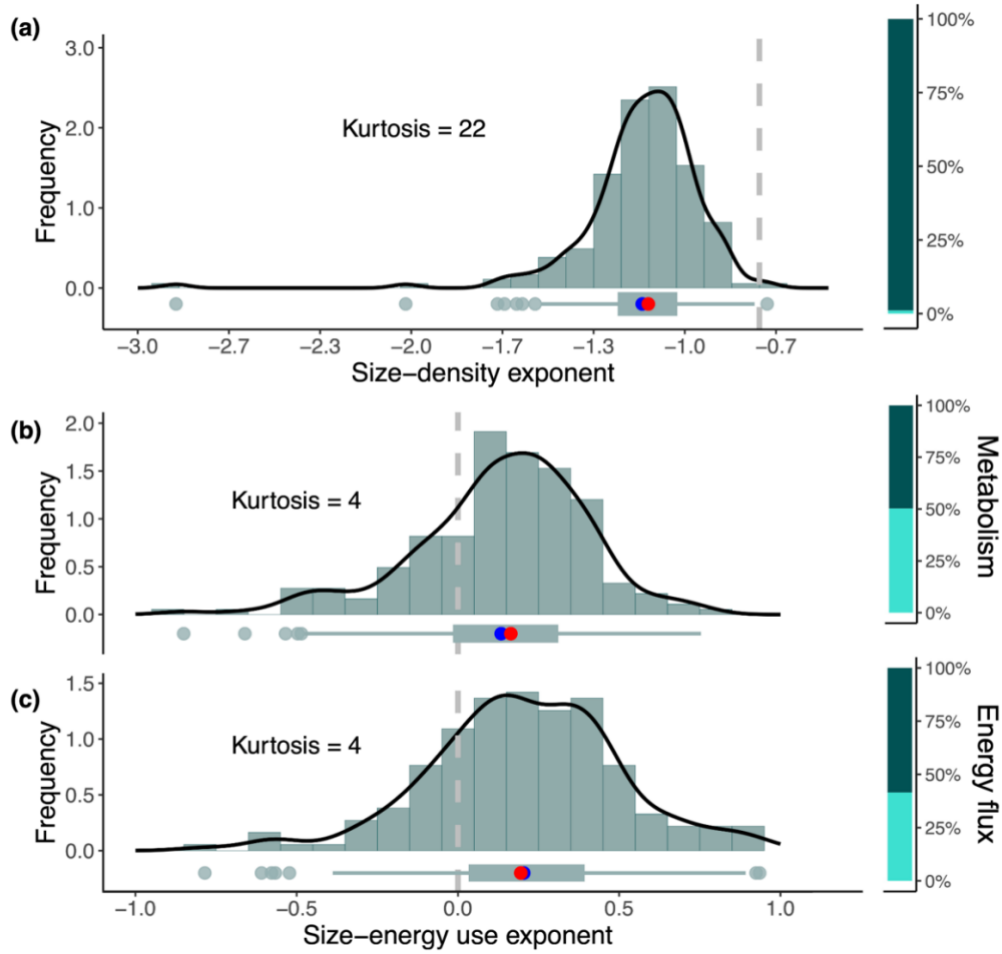


**Figure 3.** Density distributions of exponent estimates for population (a) size–density, (b) body size–metabolism, and (c) body size–energy flux relationships, with probability density functions (black line) of invertebrate consumers across whole soil food webs. Grey dashed lines indicate a size–density exponent of  $-0.75$  ( $N \propto M^{-0.75}$ ) in panel (a) and a size–energy use exponent of zero ( $E_n \propto M_n^0$ ) in panels (b) and (c). Box plots show distributions of scaling exponent values where the mean (blue dot) and median (red dot) of exponent estimates from the 183 food web–level scaling models are shown. Stacked bar plots on the right show the percentage of food webs that met (light teal) and did not meet (dark teal)  $N \propto M^{-0.75}$ ,  $I_n \propto M_n^0$ , and  $F_n \propto M_n^0$  expectations.

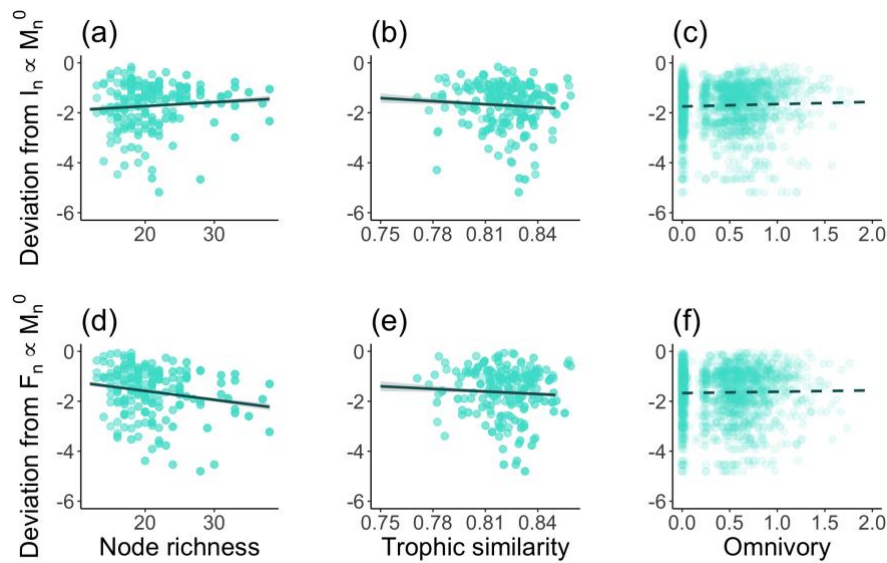


**Figure 4.** Marginal effects of node richness (i.e., number of nodes per food web, (a) & (d)), trophic similarity (similarity between nodes per food web, (b) & (e)), and omnivory (across trophic levels, (c) & (f)) on the absolute logarithm–deviation of food webs from predicted size–metabolism ( $I_n \propto M_n^0$ , top row) or size–energy flux ( $F_n \propto M_n^0$ , bottom row) exponents for all food webs. Regression lines show the relationship between each predictor variable (node richness, mean trophic similarity, and omnivory) and response variable (deviation from EER expectations) if all other predictors are held constant at their means. Dashed and solid lines denote non–significant ( $p$ -value  $> 0.05$ ) and significant ( $p$ -value  $< 0.05$ ) effects, respectively (with 95% confidence intervals shown for significant relationships). See Table S4 for model coefficients.

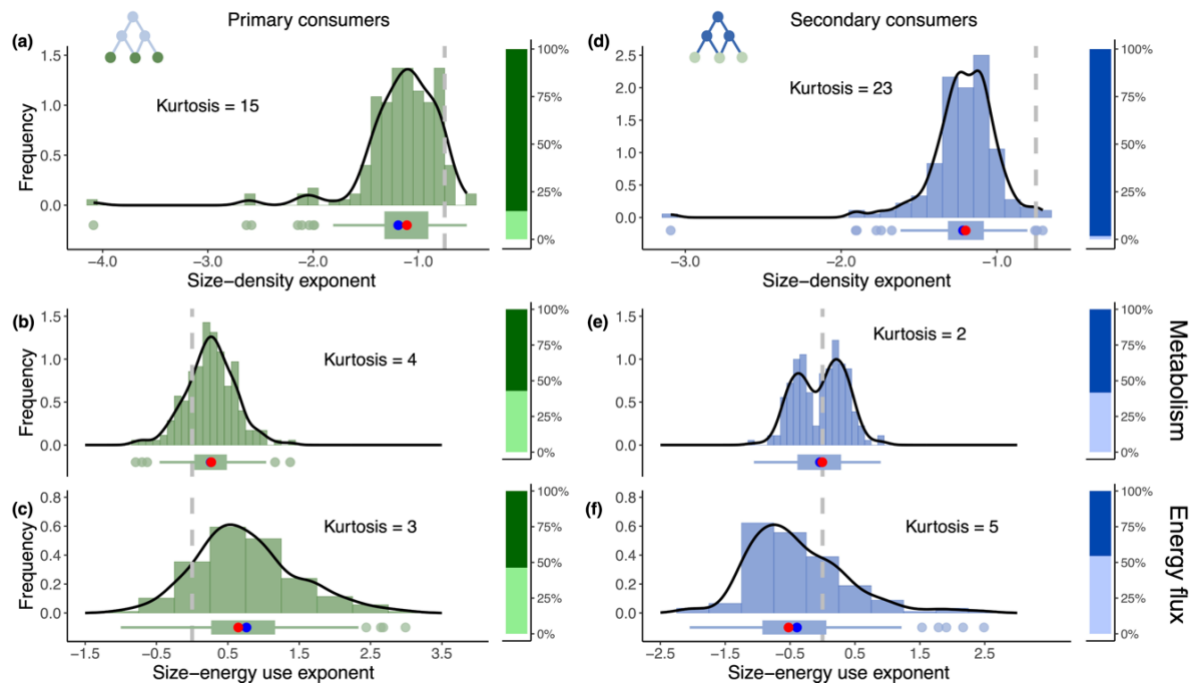


**Figure 5.** Density distributions of exponent estimates for population (a) size–density, (b) body size–metabolism, and (c) body size–energy flux relationships, with density functions (black line) for primary (green) and secondary (blue) consumer invertebrates in soil food webs. Grey dashed lines indicate a size–density exponent of  $-0.75$  ( $N \propto M^{-0.75}$ ) in panels (a) and (d) and a size–energy use exponent of zero ( $E_n \propto M_n^0$ ) in the other panels. Box plots show the distribution of scaling exponent estimates where mean (blue dot) and median (red dot) of exponent estimates from the 352 trophic–level scaling models are shown. Stacked bar plots on the right show the percentage of food webs that met (light green or blue) and did not meet (dark green or blue)  $N \propto M^{-0.75}$ ,  $I_n \propto M_n^0$ , and  $F_n \propto M_n^0$  expectations.

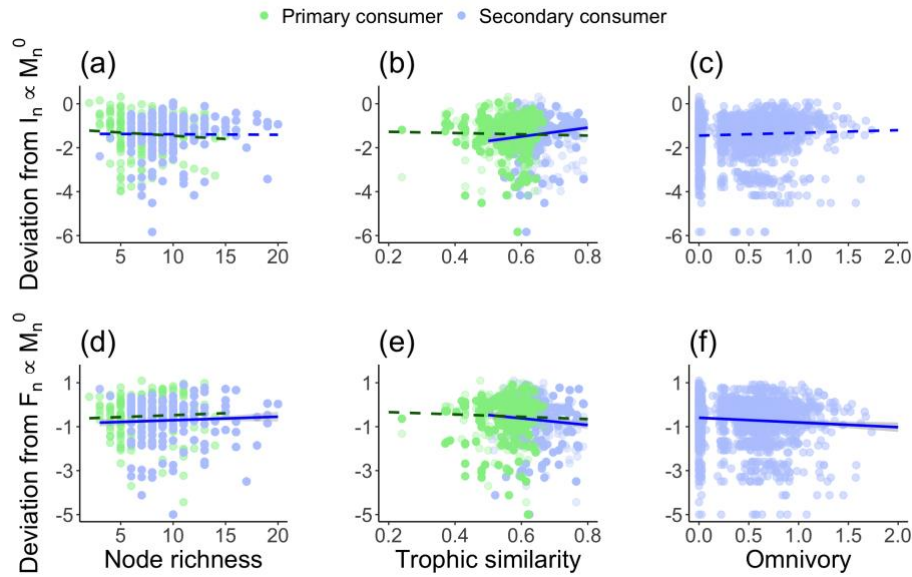


**Figure 6.** Marginal effects of node richness (i.e., number of nodes per food web, (a) & (d)), trophic similarity (similarity between nodes per food web, (b) & (e)), and omnivory (across trophic levels, (c) & (f)) on the natural logarithm–deviation of food webs from predicted size–metabolism ( $I_n \propto M_n^0$ , upper row) or size–energy flux ( $F_n \propto M_n^0$ , lower row) exponents for all primary (green) and secondary (blue) consumer food webs. Regression lines show the relationship between each predictor variable (node richness, mean trophic similarity, and omnivory) and response variable (deviation from EER expectations) where all other predictors are held constant at their means. Dashed and solid lines denote non–significant ( $p$ –value  $> 0.05$ ) and significant ( $p$ –value  $< 0.05$ ) effects, respectively (with 95% confidence intervals shown by the grey shading bands for significant relationships). Note, there is no omnivory present within the primary consumer trophic level. See Table S4 for model coefficients.

## Acknowledgements

Our project was supported by the Marsden Fund Council from Government funding managed by Royal Society Te Apārangi (grant MFP-23-UOW-029), and the People, Cities, and Nature research programme (Ministry of Business, Innovation and Employment, grant UOWX2101).

We thank the numerous people that assisted in the field and laboratory and mana whenua (indigenous people) of the land our sites were on. We acknowledge the use of data drawn from the EFForTS and ECOWORM projects. All authors gratefully acknowledge the support of iDiv, which is funded by the German Research Foundation (DFG - FZT 118, 202548816). N.E. and O.F. thank the DFG (Ei 862/29–1; Ei 862/31–1) for funding. Figure 1, and Figure 2 were created with BioRender.com. A.P. was funded by the Deutsche Forschungsgemeinschaft (DFG, German Research Foundation) – Projektnummer 493345801.

## References

- Antunes, A. C., Gauzens, B., Brose, U., Potapov, A. M., Jochum, M., Santini, L. *et al.* (2023). Environmental drivers of local abundance–mass scaling in soil animal communities. *Oikos*, 2023(2), e09735.
- Barnes, A. D., Jochum, M., Lefcheck, J. S., Eisenhauer, N., Scherber, C., O’Connor, M. I. *et al.* (2018). Energy Flux: The Link between Multitrophic Biodiversity and Ecosystem Functioning. *Trends in Ecology & Evolution*, 33(3), 186–197.
- Barnes, A. D., Jochum, M., Mumme, S., Haneda, N. F., Farajallah, A., Widarto, T. H. *et al.* (2014). Consequences of tropical land use for multitrophic biodiversity and ecosystem functioning. *Nature Communications*, 5(1), 5351.
- Barnes, A. D., Scherber, C., Brose, U., Borer, E. T., Ebeling, A., Gauzens, B. *et al.* (2020). Biodiversity enhances the multitrophic control of arthropod herbivory. *Science Advances*, 6(45), eabb6603.
- Brown, J. H., Gillooly, J. F., Allen, A. P., Savage, V. M., West, G. B. (2004). Toward a metabolic theory of ecology. *Ecology*, 85(7), 1771–1789.
- Damuth, J. (1981). Population density and body size in mammals. *Nature*, 290(5808), 699–700.

- Damuth, J. (1987). Interspecific allometry of population density in mammals and other animals: The independence of body mass and population energy–use. *Biological Journal of the Linnean Society*, 31(3), 193–246.
- Drescher, J., Rembold, K., Allen, K., Beckschäfer, P., Buchori, D., Clough, Y. *et al.* (2016). Ecological and socio–economic functions across tropical land use systems after rainforest conversion. *Philosophical Transactions of the Royal Society B: Biological Sciences*, 371(1694), 20150275.
- Edwards, A. M., Robinson, J. P. W., Plank, M. J., Baum, J. K., Blanchard, J. L. (2017). Testing and recommending methods for fitting size spectra to data. *Methods in Ecology and Evolution*, 8(1), 57–67.
- Ehnes, R. B., Pollierer, M. M., Erdmann, G., Klarner, B., Eitzinger, B., Digel, C. *et al.* (2014). Lack of energetic equivalence in forest soil invertebrates. *Ecology*, 95(2), 527–537.
- Ehnes, R. B., Rall, B. C., Brose, U. (2011). Phylogenetic grouping, curvature and metabolic scaling in terrestrial invertebrates: Invertebrate metabolism. *Ecology Letters*, 14(10), 993–1000.
- Eisenhauer, N. (2012). Aboveground–belowground interactions as a source of complementarity effects in biodiversity experiments. *Plant and Soil*, 351(1-2), 1–22.
- Gauzens, B., Barnes, A., Giling, D. P., Hines, J., Jochum, M., Lefcheck, J. S. *et al.* (2019). *fluxweb*: An R package to easily estimate energy fluxes in food webs. *Methods in Ecology and Evolution*, 10(2), 270–279.
- Glazier, D. S. (2022). Variable metabolic scaling breaks the law: From ‘Newtonian’ to ‘Darwinian’ approaches. *Proceedings of the Royal Society B: Biological Sciences*, 289(1985), 20221605.

- Hatton, I. A., Dobson, A. P., Storch, D., Galbraith, E. D., Loreau, M. (2019). Linking scaling laws across eukaryotes. *Proceedings of the National Academy of Sciences*, 116(43), 21616–21622.
- Hechinger, R. F., Lafferty, K. D., Dobson, A. P., Brown, J. H., Kuris, A. M. (2011). A Common Scaling Rule for Abundance, Energetics, and Production of Parasitic and Free-Living Species. *Science*, 333(6041), 445–448.
- Jochum, M., Ferlian, O., Thakur, M. P., Ciobanu, M., Klarner, B., Salamon, J. *et al.* (2021). Earthworm invasion causes declines across soil fauna size classes and biodiversity facets in northern North American forests. *Oikos*, 130(5), 766–780.
- Johnston, A. S. A., & Sibly, R. M. (2020). Multiple environmental controls explain global patterns in soil animal communities. *Oecologia*, 192(4), 1047–1056.
- Marquet, P. A., Navarrete, S. A., Castilla, J. C. (1995). Body Size, Population Density, and the Energetic Equivalence Rule. *The Journal of Animal Ecology*, 64(3), 325.
- Meehan, T. D. (2006a). Energy use and animal abundance in litter and soil communities. *Ecology*, 87(7), 1650–1658.
- Meehan, T. D. (2006b). Mass and temperature dependence of metabolic rate in litter and soil invertebrates. *Physiological and Biochemical Zoology*, 79(5), 878–884.
- Meehan, T. D., Drumm, P. K., Schottland, F. R., Oral, K., Lanier, K. E., Pennington, E. A. *et al.* (2006). Energetic equivalence in a soil arthropod community from an aspen–conifer forest. *Pedobiologia*, 50(4), 307–312.
- Mercer, R. D., Gabriel, A. G. A., Barendse, J., Marshall, D. J., Chown, S. L. (2001). Invertebrate body sizes from Marion Island. *Antarctic Science*, 13(2), 135–143.
- National Oceanic and Atmospheric Administration. (n.d.). *NOWData*. National Weather Service. <https://w2.weather.gov/climate/xmacis.php?wfo=mpx>

- Naumann, I. D. (1991). *The Insects of Australia: A textbook for students and research workers: Free Download, Borrow, and Streaming: Internet Archive*. Carlton, Vic.: Melbourne University Press.  
<https://archive.org/details/insectsofaustral0002unse/mode/2up>
- Petersen, H., & Luxton, M. (1982). A Comparative Analysis of Soil Fauna Populations and Their Role in Decomposition Processes. *Oikos*, 39(3), 288.
- Poisot, T., Mouquet, N., Gravel, D. (2013). Trophic complementarity drives the biodiversity–ecosystem functioning relationship in food webs. *Ecology Letters*, 16(7), 853–861.
- Polis, G. A., & Strong, D. R. (1996). Food Web Complexity and Community Dynamics. *The American Naturalist*, 147(5), 813–846.
- Potapov, A. M., Beaulieu, F., Birkhofer, K., Bluhm, S. L., Degtyarev, M. I., Devetter, M. *et al.* (2022), Feeding habits and multifunctional classification of soil–associated consumers from protists to vertebrates. *Biol Rev*, 97: 1057–1117.
- Potapov, A. M., Brose, U., Scheu, S., Tiunov, A. V. (2019a). Trophic Position of Consumers and Size Structure of Food Webs across Aquatic and Terrestrial Ecosystems. *The American Naturalist*, 194(6), 823–839.
- Potapov, A. M., Klärner, B., Sandmann, D., Widayastuti, R., Scheu, S. (2019b). Linking size spectrum, energy flux and trophic multifunctionality in soil food webs of tropical land-use systems. *Journal of Animal Ecology*, 88(12), 1845–1859.
- Potapov, A. M., Rozanova, O. L., Semenina, E. E., Leonov, V. D., Belyakova, O. I., Bogatyreva, V. Yu. *et al.* (2021). Size compartmentalization of energy channeling in terrestrial belowground food webs. *Ecology*, 102(8), e03421.
- R Core Team. (2023). *R: A Language and Environment for Statistical Computing* [Computer software]. R Foundation for Statistical Computing. <https://www.R-project.org/>

- Savage, V. M., Gillooly, J. F., Woodruff, W. H., West, G. B., Allen, A. P., Enquist, B. J. *et al.* (2004). The predominance of quarter–power scaling in biology. *Functional Ecology*, 18(2), 257–282.
- Sohlström, E. H., Marian, L., Barnes, A. D., Haneda, N. F., Scheu, S., Rall, B. C. *et al.* (2018). Applying generalized allometric regressions to predict live body mass of tropical and temperate arthropods. *Ecology and Evolution*, 8(24), 12737–12749.
- Trebilco, R., Baum, J. K., Salomon, A. K., Dulvy, N. K. (2013). Ecosystem ecology: Size–based constraints on the pyramids of life. *Trends in Ecology & Evolution*, 28(7), 423–431.
- Ulrich, W., Hoste–Danyłow, A., Faleńczyk–Koziróg, K., Hajdamowicz, I., Ilieva–Makulec, K., Olejniczak, I. *et al.* (2015). Temporal patterns of energetic equivalence in temperate soil invertebrates. *Oecologia*, 179(1), 271–280.
- White, E. P., Ernest, S. K. M., Kerkhoff, A. J., Enquist, B. J. (2007). Relationships between body size and abundance in ecology. *Trends in Ecology & Evolution*, 22(6), 323–330.

## Supplementary

**Table S1.** Plot information for the urban forest plots throughout Aotearoa New Zealand for acquiring aboveground (tree) and belowground (invertebrate) data.

Plot name	City	Year planted	Patch size (ha)	Latitude–longitude
Aynsley terrace	Christchurch	1990	0.43	–43.562168, 172.662834
Halswell quarry	Christchurch	2001	0.43	–43.598476, 172.574855
Marshland road	Christchurch	2006	0.49	–43.45122, 172.663124
Matawai	Christchurch	1975	0.44	–43.31616, 172.594527
Radcliffe road	Christchurch	2011	1.70	–43.465107, 172.649435
Riccarton bush	Christchurch	1979	9.65	–43.526368, 172.59772
Styx living lab	Christchurch	2003	0.27	–43.45449, 172.664372
Travis wetland	Christchurch	2000	0.27	–43.48653, 172.697303
Wigram east	Christchurch	1993	0.81	–43.555706, 172.578838
Craigieburn intermediate	Dunedin	2000	18.00	–45.841772, 170.495005
Craigieburn old	Dunedin	1960	18.00	–45.841393, 170.494362
Craigieburn young	Dunedin	2011	18.00	–45.841487, 170.495108
Frasers gully	Dunedin	2003	0.98	–45.863073, 170.470193
Island park	Dunedin	2009	77.30	–45.552702, 170.24387
Prospect park	Dunedin	1997	18.80	–45.856111, 170.508141
Signal hill	Dunedin	1989	148.00	–45.857614, 170.547932
Upper Leith walkway	Dunedin	1997	18.80	–45.852453, 170.504709
Avalon	Hamilton	2006	0.46	–37.770445, 175.241399

Brymer	Hamilton	1996	1.10	−37.782203, 175.2266
Claudeland remnant	Hamilton	old–growth	6.05	−37.77433, 175.290224
Featherstone park	Hamilton	2001	0.10	−37.733648, 175.237567
Hamilton lake	Hamilton	1999	3.20	−37.79246, 175.27458
Minogue	Hamilton	1980	2.44	−37.773849, 175.249727
Tauhara	Hamilton	1988	0.83	−37.743952, 175.26376
Tills	Hamilton	1995	0.40	−37.802819, 175.233042
Waiwhakareke old	Hamilton	2005	1.32	−37.771058, 175.224813
Waiwhakareke young	Hamilton	2012	7.95	−37.770819, 175.220964
Bushy point young	Invercargill	2006	27.00	−46.446669, 168.318588
Estuary walkway	Invercargill	1997	0.99	−46.427467, 168.343241
Kew bush	Invercargill	1999	3.79	−46.440169, 168.359376
Kew bush remnant	Invercargill	old–growth	3.79	−46.440725, 168.358204
Rance covenant old	Invercargill	1996	27.00	−46.45131, 168.317501
Rance covenant young	Invercargill	2000	27.00	−46.45077, 168.318031
Thomsons bush exterior	Invercargill	2011	20.90	−46.381121, 168.354084
Thomsons bush interior	Invercargill	2009	20.90	−46.383404, 168.359923
Waihopi river	Invercargill	2007	0.10	−46.388762, 168.350195
Bobs track	Nelson	1989	5.00	−41.282856, 173.256909
Murphy reserve old	Nelson	2001	1.65	−41.286782, 173.263165
Murphy reserve young	Nelson	2010	1.65	−41.285237, 173.263615
Newman grove	Nelson	1990	0.11	−41.258883, 173.296274

Pipers reserve	Nelson	2012	13.20	-41.285939, 173.258375
Titoki	Nelson	2005	31.80	-41.237767, 173.327055
Waste station	Nelson	1990	0.22	-41.292933, 173.240344
Whakatu drive	Nelson	2002	1.90	-41.306908, 173.220461
Whitehead park	Nelson	1998	20.30	-41.26586, 173.300401
Airport	New Plymouth	1990	1.31	-39.030298, 174.166158
Herekawe coastal	New Plymouth	2014	8.90	-39.070439, 174.021828
Herekawe inland	New Plymouth	2002	2.71	-39.076651, 174.028247
Huatoki restored	New Plymouth	1972	30.00	-39.083646, 174.0763
Peringa park	New Plymouth	2006	1.19	-39.042496, 174.111815
Pukekura park	New Plymouth	2008	18.80	-39.072779, 174.087731
Salaman reserve	New Plymouth	1991	4.26	-39.079247, 174.064327
Te henui	New Plymouth	2005	12.00	-39.072776, 174.096182
Waipu lagoon	New Plymouth	1988	1.49	-39.030211, 174.137023
Bethlehem	Tauranga	1997	2.82	-37.696373, 176.124102
Carmichael playground	Tauranga	2007	1.36	-37.688042, 176.121437
Challenge reserve	Tauranga	2004	2.13	-37.701165, 176.138539
Johnson reserve	Tauranga	1996	14.90	-37.732759, 176.177179
McCardles bush	Tauranga	1987	9.86	-37.678491, 176.147211
Millbrook	Tauranga	2002	4.75	-37.697815, 176.122643
Ohauiti intermediate	Tauranga	2004	0.32	-37.749361, 176.159434
Ohauiti old	Tauranga	2001	0.10	-37.746789, 176.16062

Ohauiti young	Tauranga	2013	4.37	-37.745879, 176.160671
Alexandra road	Wellington	2000	18.50	-41.303117, 174.789812
Izard park	Wellington	1996	3.32	-41.264276, 174.763242
Manawa Kariori north	Wellington	1991	2.64	-41.330492, 174.768949
Manawa Kariori south	Wellington	1991	2.64	-41.330897, 174.768432
Mt. Albert	Wellington	1992	7.34	-41.329203, 174.782078
Old chest hospital	Wellington	2010	3.19	-41.307502, 174.786127
Otari wilton remnant	Wellington	old-growth	237	-41.267091, 174.758319
Owen street	Wellington	2010	14.90	-41.316814, 174.787255
Tawatawa reserve	Wellington	1994	2.99	-41.334565, 174.761012
Telford terrace	Wellington	2004	8.77	-41.292255, 174.796332

**Table S2.** Equations for calculating body size (M, mg) from organism body length (L, mm) or dry size (DM, mg) for the Aotearoa New Zealand data.

Class	Order	Sub cohort	Life stage	Equation	a	b	Source
Arachnida	Prostigmata	Anystina					Mercer et al. 2001
		Eupodina		$(10^{(2.124+2.808*\log(L))})/1000$			
		Heterostigmata					
		Parasitengonina					
		Raphignathina					
	Oribatida			$(10^{(2.117+2.711*\log(L))})/1000$			
	Mesostigmata			$(10^{(2.064+2.857*\log(L))})/1000$			
Entognatha	Collembola			$(10^{(1.339+1.992*\log(L))})/1000$			Mercer et al. 2001

Diplura				$10^{(-1.316+2.529*\log(L))}$			Barnes et al. 2014; Sohlström et al. 2018
Symphyla				$10^{(-2.917+2.837*\log_{10}(L))}$			Barnes et al. 2014; Sohlström et al. 2018
Class	Order	Family	Life stage	Equation	a	b	Source
Arachnida	Araneae		Adult	$10^{(a + (b * \log_{10}(L)))}$	-0.830	2.637	Barnes et al.
	Opiliones		Adult		-0.385	2.439	2014; Sohlström et al. 2018
	Pseudoscorpiones		Adult		0.942	2.015	
Chilopoda			Adult	$10^{(a + (b * \log_{10}(L)))}$	-2.917	2.837	Barnes et al. 2014; Sohlström et al. 2018

Clitellata	Haplotaxida	Adult	$\text{EXP}(a + b * \log(\text{DM}))$	0.9282	1.0899	Mercer et al. 2001
Diplopoda		Adult	$10^{(a + (b * \log_{10}(L)))}$	-1.986	2.944	Barnes et al. 2014; Sohlström et al. 2018
Insecta	Thysanoptera	Adult	$\text{EXP}(a + b * \log(\text{DM}))$	0.6111	1.0213	Mercer et al. 2001
	Blattodea	Nymph				
	Coleoptera	Grub	$10^{(a + (b * \log_{10}(L)))}$	-1.888	2.934	Barnes et al. 2014; Sohlström et al. 2018
		Tenebrionidae	Larvae	-1.229	2.244	Mercer et al. 2001; Sohlström et al. 2018
		Curculionidae	Larvae			
		Staphylinidae	Larvae			

	Elateridae	Larvae				
	Cryptophagidae	Larvae				
	Staphylinidae	Adult		-1.053	2.592	Barnes et al.
	Curculionidae	Adult				2014; Sohlström
	Elateridae	Adult				et al. 2018
	Cryptophagidae	Adult				
	Tenebrionidae	Adult				
	Nitidulidae	Adult				
	Latridiidae	Adult				
	Curculionidae	Adult				
	Carabidae	Adult				
	Mycetophagidae	Adult				
Dermaptera		Adult	$10^{(a + (b * \log_{10}(L)))}$	1.316	2.529	Barnes et al.
						2014; Sohlström
						et al. 2018

Diptera	Chironomidae	Larvae	$M = 10^{(-a + (b * \log_{10}(L)))}$	-1.229	2.244	Mercer et al.
	Therevidae	Larvae				2001; Sohlström
	Calliphoridae	Larvae				et al. 2018
	Tephritidae	Larvae				
	Platypezidae	Larvae	$10^{(a + (b * \log_{10}(L)))}$	-1.229	2.244	
	Mycetophilidae	Adult		-1.032	2.43	
Psocodea		Adult	$10^{(a + (b * \log_{10}(L)))}$	-1.154	2.71	Mercer et al.
						2001; Sohlström
						et al. 2018
Hemiptera	Aphididae	Adult		0.817	2.237	Barnes et al.
Hymenoptera	Formicidae	Adult		-1.38	2.712	2014; Sohlström
Neuroptera	Hemerobiidae	Adult		-0.871	2.01	et al. 2018
Orthoptera		Adult		0.791	2.245	
Malacostraca	Amphipoda	Talitridae	Adult	$10^{(a + (b * \log_{10}(L)))}$	-1.322	2.967

Isopoda	Armadillidiidae	Adult				Barnes et al. 2014; Sohlström et al. 2018
Turbellaria		Adult	$10^{(a + (b \cdot \log_{10}(L)))}$	-2.917	2.837	Barnes et al. 2014; Sohlström et al. 2018

1 **Table S3.** Regression model fit values applied to equation 1 for each taxon from Ehnes et al.  
 2 (2011). Where  $\ln i_0$  = natural logarithm normalisation factor,  $\alpha$  = allometric exponent, E =  
 3 activation energy.

Regression group	$\ln i_0$	$\alpha$	E
Oribatida	22.023	0.679	0.706
Mesostigmata	9.674	0.690	0.379
Prostigmata	10.281	0.660	0.413
Arachnida	24.581	0.565	0.709
Coleoptera	21.418	0.738	0.639
Insecta	21.972	0.759	0.657
Hymenoptera	22.013	0.742	0.668
Isopoda	23.169	0.554	0.687
Chilopoda	28.253	0.558	0.803
Clitellata	12.442	0.801	0.443
Progoneata	22.347	0.571	0.670
General	23.055	0.695	0.686

4

#### 5 **Food web reconstruction and consumer energy flux calculation**

6 Using the fluxing function from the fluxweb package in R (Gauzens et al. 2019), the influx of  
 7 energy to consumer ( $j$ ) was calculated as:

$$8 \quad 1) \quad \sum_i (W_{ij} \times e_{ij} \times F_{ij}) = I_j + \sum_j (W_{ij} \times F_j)$$

9 where  $e_{ij}$  is the assimilation efficiency by which a consumer ( $j$ ) converts energy consumed  
 10 from its resource ( $i$ ) into energy for metabolism and biomass production. To determine the  
 11 assimilation efficiency of energy by consumers based on the resources they feed on,  $e_{ij}$  for

12 animals (e.g., as resources of predators) was set to 0.906, plants to 0.545, detritus 0.158  
13 (Barnes et al. 2020; Lang et al. 2017), bacteria 0.6, and fungi 0.5 (De Ruiter et al. 1993).  
14 Metabolic rate  $I_j$  for all animal consumers was equal to the summed individual metabolic  
15 rates per node, per plot.  $I_j$  for all basal resources (bacteria, detritus, plants, and fungi) was set  
16 to 1 following Barnes et al. (2020).  $F_{ij} = W_{ij} \times F_j$  is the flux of energy to a consumer where  $F_j$   
17 is the sum of fluxes into a node and  $W_{ij}$  is the proportion of  $F_j$  obtained by the node according  
18 to scaled consumer preferences ( $w_{ij}$ ) to the biomasses of different available prey as:

$$19 \quad 2) \quad W_{ij} = w_{ij} \times B_i / \sum_j w_{ij} \times B_j$$

20 where  $B_i$  and  $B_j$  is the resource and consumer biomass, respectively.  $B_i$  for all animal  
21 resources and  $B_j$  for all animal consumers were equal to the summed fresh body masses (mg)  
22 of all individuals per node type, per plot (Barnes et al. 2020). All basal resource biomasses  
23 were set to be equal to the average biomass of all consumer node types per plot to set near-  
24 equal preferences of omnivores between predatory links and basal resources. This was done  
25 to reduce extreme preferences of omnivores towards basal resources such as plants and  
26 detritus that typically have much higher biomasses compared to soil invertebrate prey, but are  
27 less preferred by them as they are lower in nutritional value. Barnes et al. (2020) tested  
28 whether the assignment of feeding preferences of omnivores between basal resources (in this  
29 case, just plants) and animals could affect energy fluxes by altering feeding preferences for  
30 plants between 0.2 to 0.9 and found no significant change in the outcome of their analysis;  
31 therefore, we set equal preferences between basal resources and animal prey in our food  
32 webs. Additionally, to reduce the amount of energy predators consume from their own  
33 biomass pool and unrealistic feeding preferences towards cannibalism, we set the feeding  
34 preferences of any cannibalistic links to 0.1.

35

36 To obtain food web metrics that could explain variation in expectations of size–density  
37 scaling and energetic equivalence of soil food webs, we quantified mean trophic similarity  
38 among nodes (for the whole food web, and within primary and secondary consumers) by  
39 calculating the average Jaccard similarity among consumer nodes based on their feeding links  
40 with resource nodes. High trophic similarity indicates a large average overlap among  
41 consumers, which can occur in the absence of omnivory, e.g. if many specialists feed on a  
42 shared resource. We calculated observed node richness as the number of nodes within each  
43 food web (total nodes in the food web, and the number of primary and secondary consumer  
44 nodes). Furthermore, we calculated trophic level omnivory of secondary consumer  $i$  ( $O_i$ ) as  
45 the variance of the trophic levels of its prey:

$$46 \quad 3) \quad O_i = 1 / n_i \sum_{j=1 \dots n_i} (TL_j - TL_{\bar{x}i})^2$$

47 Where  $TL_{\bar{x}i}$  is the average trophic level of the prey of species  $i$ .

48

49 For each local food web, we further determined the prey–averaged trophic level ( $TL_i$ ) of each  
50 node, such that the trophic level was equal to one for basal resources, two for primary  
51 consumers, and  $> 2$  for secondary consumers as:

$$52 \quad 4) \quad TL_i = 1 / n_i \sum_{j=1 \dots n_i} TL_j$$

53 Where  $n_i$  is the number of prey of species  $i$ , and  $j$  are prey of species  $i$ .

54

## 55 **Statistical analysis**

56 To analyse size–metabolism ( $I_n \propto M_n$ ), and size–energy flux ( $F_n \propto M_n$ ) scaling relationships  
57 across whole soil invertebrate food webs and within primary and secondary consumers, we  
58 also used ranged major axis (RMA) regression using the ‘lmodel2’ package in R to analyse  
59 these relationships (see Fig. S1 & S2 for  $I_n \propto M_n$  and  $F_n \propto M_n$  regressions using RMA  
60 regression; Legendre, 2018). RMA regression is used when both x and y variables (e.g.,

61 median body size, abundance, metabolism, and energy flux) in the regression equation are  
 62 random (Legendre, 2018). RMA regression models were run across all communities (i.e.,  
 63 plots) within the four geographic regions. We excluded all resulting models with less than 10  
 64 body size class bins or individuals per food web from our analysis due to insufficient data for  
 65 estimating reliable model fits. As a result, our analyses yielded a total of 183 food webs (i.e.,  
 66 comprising both primary and secondary consumers) and 360 trophic level models (180  
 67 models for primary consumers and 180 for secondary consumer food webs).

68

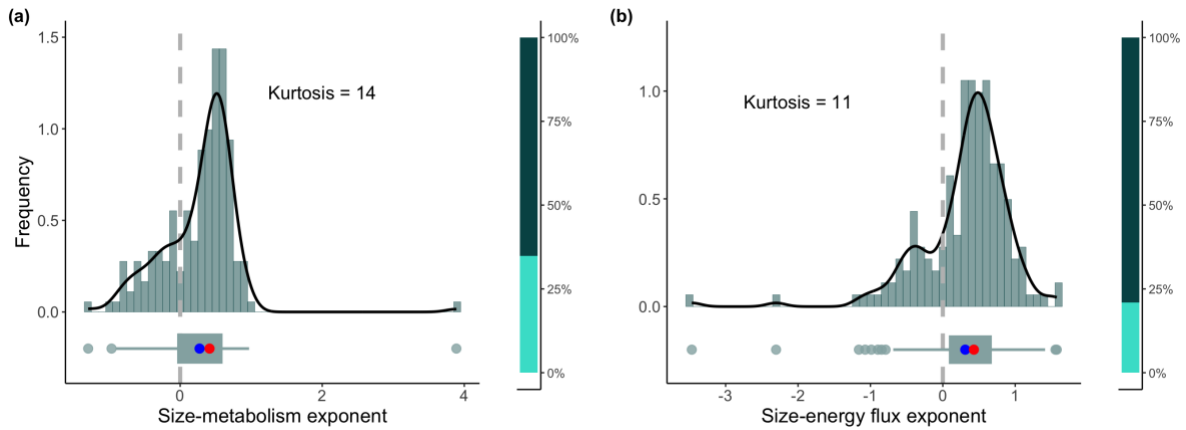
69 **Table S4.** Coefficients table corresponding to the marginal effects models of node richness  
 70 and trophic similarity on the natural logarithm–deviation of food webs from predicted  $I_n \propto M_n^0$   
 71 or  $F_n \propto M_n^0$  exponents for all food webs, overall and for primary (PC) and secondary  
 72 consumers (SC; shown in Fig. 4 and Fig. 6 in main text). ‘Std.Error’ is standard error, ‘ $p$ ’ is  
 73  $p$ -value, and ‘DF’ is degrees of freedom. Note, there is no omnivory present within the  
 74 primary consumer trophic levels.

	Exponent	Std. Error	t-value	$p$	DF
Overall $I_n \propto M_n^0$ deviation					1,798
Intercept	2.420	0.887	2.727	0.01	
Node richness	0.008	0.003	2.460	0.01	
Trophic similarity	-4.327	1.088	-3.978	<0.01	
Omnivory	0.036	0.050	0.720	0.47	
Overall $F_n \propto M_n^0$ deviation					1,798
Intercept	2.675	0.876	3.054	<0.01	
Node richness	-0.055	0.003	-17.281	<0.01	
Trophic similarity	-2.883	1.073	-2.686	0.01	
Omnivory	-0.013	0.049	-0.268	0.79	

PC $I_n \propto M_n^0$ deviation					170
Intercept	-0.197	0.413	-0.477	0.63	
Node richness	0.026	0.021	1.246	0.21	
Trophic similarity	-0.99	0.830	-1.193	0.24	
Omnivory	NA	NA	NA	NA	
PC $F_n \propto M_n^0$ deviation					170
Intercept	-0.149	0.523	-0.285	0.78	
Node richness	0.146	0.027	5.465	<0.01	
Trophic similarity	-0.943	1.051	-0.897	0.37	
Omnivory	NA	NA	NA	NA	
SC $I_n \propto M_n^0$ deviation					1593
Intercept	-1.905	0.213	-8.943	<0.01	
Node richness	-0.015	0.008	-1.93	0.05	
Trophic similarity	2.033	0.409	4.971	<0.01	
Omnivory	0.155	0.048	3.266	<0.01	
SC $F_n \propto M_n^0$ deviation					1,593
Intercept	1.203	0.264	4.550	<0.01	
Node richness	0.128	0.010	13.372	<0.01	
Trophic similarity	-2.807	0.508	-5.529	<0.01	
Omnivory	-0.026	0.059	-0.435	0.66	

75

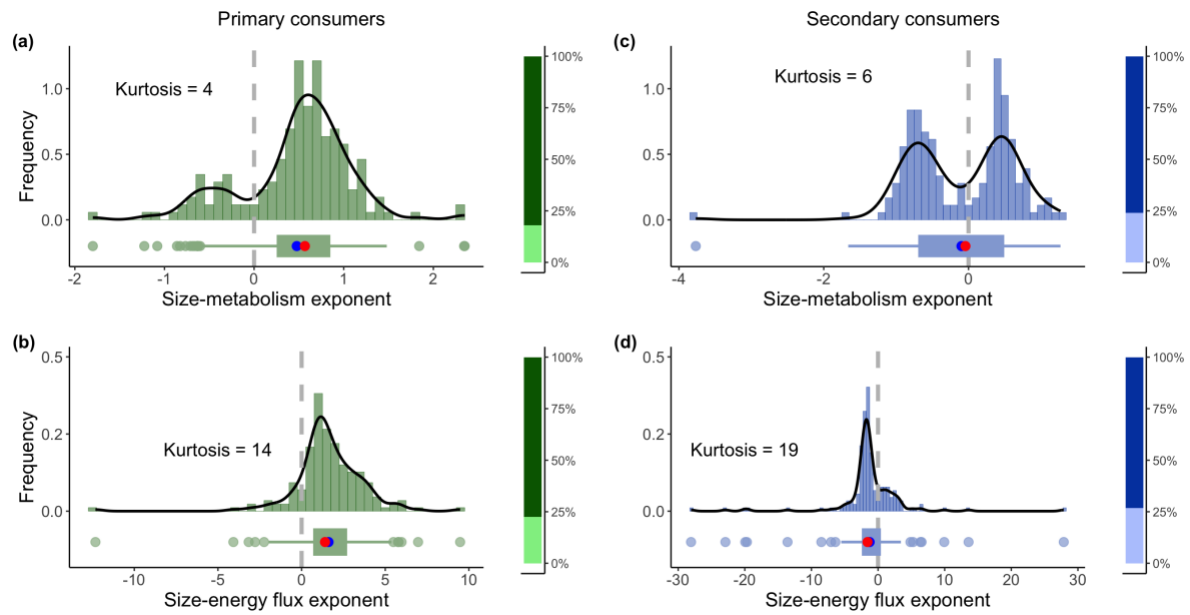
76



77

78 **Figure S1.** Density distributions of exponent estimates for natural logarithm–transformed  
 79 median body size–metabolism (a), and natural logarithm–transformed median body size–  
 80 energy flux (b) relationships, with probability density functions (black line) of invertebrate  
 81 consumers across whole soil food webs using ranged major axis regression. Grey dashed line  
 82 indicates a size–energy use exponent of zero ( $E_n \propto M_n^0$ ). Box plots showing scaling exponent  
 83 values distribution where mean (blue dot) and median (red dot) of exponent estimates from  
 84 the 183 food web–level scaling models are shown.  $I_n \propto M_n$  (mean = 0.273, median = 0.414)  
 85 and  $F_n \propto M_n$  (mean = 0.310, median = 0.429). Out of 183 soil food webs, 34.8% met  $I_n \propto M_n^0$ ,  
 86 and 21% met  $F_n \propto M_n^0$  expectations. Stacked bar plots on the right show the percentage of  
 87 food webs that met  $I_n \propto M_n^0$  and  $F_n \propto M_n^0$  expectations for each row of panels. Note, two food  
 88 webs (i.e., RMA models) were identified as statistical outliers and removed as they had  
 89 exponents of up to two orders of magnitude greater than all other exponents, as well as  
 90 having extremely large p–values. Inclusion of these two food webs also resulted in models  
 91 violating assumptions of homogeneity of variance and normality in subsequent analyses,  
 92 providing further justification for their exclusion. As a result, our analyses yielded a total of  
 93 543 models (183 models each for whole food webs, for primary consumers, and for  
 94 secondary consumers).

95



96

97 **Figure S2.** Density distributions of exponent estimates for natural logarithm–transformed  
 98 median body size–metabolism (a & c), and natural logarithm–transformed median body size–  
 99 energy flux (b & d) relationships, with probability density functions (black line) of primary  
 100 (green) and secondary (blue) consumers across whole soil food webs using ranged major axis  
 101 regression. Grey dashed line indicates a size–energy use exponent of zero ( $E_n \propto M_n^0$ ). Box  
 102 plots showing scaling exponent values distribution where mean (blue dot) and median (red  
 103 dot) of exponent estimates from the 362 food web–level scaling models are shown.  $I_n \propto M_n$   
 104 (mean =  $-0.093$ , median =  $-0.036$ ) and  $F_n \propto M_n$  (mean =  $-1.267$ , median =  $-1.583$ ). Out of  
 105 180 primary consumer soil food webs, 17.2% met  $I_n \propto M_n^0$  and 21.7% met  $F_n \propto M_n^0$   
 106 expectations. Out of 180 secondary consumer soil food webs, 23.9% met  $I_n \propto M_n^0$  and 26.7%  
 107 met  $F_n \propto M_n^0$  expectations. Stacked bar plots on the right show the percentage of food webs  
 108 that met  $N \propto M^{-0.75}$ ,  $I_n \propto M_n^0$ , and  $F_n \propto M_n^0$  expectations for each row of panels. Note, two food  
 109 webs (i.e., RMA models) were identified as statistical outliers and removed as they had  
 110 exponents of up to two orders of magnitude greater than all other exponents, as well as  
 111 having extremely large p–values. Inclusion of these two food webs also resulted in models  
 112 violating assumptions of homogeneity of variance and normality in subsequent analyses,

113 providing further justification for their exclusion. As a result, our analyses yielded a total of  
114 543 models (183 models each for whole food webs, for primary consumers, and for  
115 secondary consumers).

116

## 117 **References**

118 Barnes, A. D., Scherber, C., Brose, U., Borer, E. T., Ebeling, A., Gauzens, B. *et al.* (2020).

119 Biodiversity enhances the multitrophic control of arthropod herbivory. *Science*  
120 *Advances*, 6(45), eabb6603.

121 De Ruiter, P. C., Van Veen, J. A., Moore, J. C., Brussaard, L., Hunt, H. W. (1993).

122 Calculation of nitrogen mineralization in soil food webs. *Plant and Soil*, 157(2), 263–  
123 273.

124 Gauzens, B., Barnes, A., Giling, D. P., Hines, J., Jochum, M., Lefcheck, J. S. *et al.* (2019).

125 *fluxweb*: An R package to easily estimate energy fluxes in food webs. *Methods in*  
126 *Ecology and Evolution*, 10(2), 270–279.

127 Lang, B., Ehnes, R. B., Brose, U., Rall, B. C. (2017). Temperature and consumer type  
128 dependencies of energy flows in natural communities. *Oikos*, 126(12), 1717–1725.

129 Legendre, P. (2018). *Model II regression user's guide, R edition*. chrome-

130 extension://efaidnbmnnnibpcajpcgclefindmkaj/https://cran.r-

131 project.org/web/packages/lmodel2/vignettes/mod2user.pdf

132